Attachment 16(f)

EVALUATION OF HYDRAULIC HEAD DATA OF SELECTED HYDROGEOLOGIC UNITS AT THE HANFORD SITE, WASHINGTON

BY

A.M. Djerrari
V.V. Nguyen
P.K. Kitanidis
EWA, Inc.

Submitted to:

YAKIMA NATION

Date:

February 6, 1987

EWA

EWA

EWA

EWA RESEARCH • ENGINEERING • PLANNING • MANAGEMENT

To : Yakima File Task VI. b
From : A. M. Djerrari, V. V. Nguyen and P. K. Kitanidis/EWA, Inc.
Subject: Evaluation of Hydraulic Head Data of Selected Hydrogeologic Units at the Hanford Site, Washington.
Date : February 6, 1987.

EXECUTIVE SUMMARY

Under the Nuclear Waste Policy Act of 1982, the U.S. Department of Energy (DOE) has been charged with identifying the site at which the first nuclear waste repository will be constructed. The Hanford Site, located in Washington, is one of the three sites (the other two being Yucca Mountain, NV and Deaf Smith County, TX) recently recommended by DOE and nominated by the President of the United States for site characterization. The ultimate goal of the site characterization is to determine the suitability of each site for deep geologic nuclear waste disposal. The important criteria in determining whether the site is suitable for the construction of a nuclear waste repository include: (1) groundwater travel time between the disturbed zone and the accessible environment; and (2) release rate of waste radionuclides to the accessible environment.

To assess and define the repository performance for licensing purposes, the DOE will make intensive use of computer modelling of the groundwater system. This requires that the groundwater flow patterns and directions in the vicinity of the proposed repository location be delineated from the hydrologic data collected at the Hanford Site.

The present study evaluates available water head elevation data for their sufficiency to provide reliable groundwater flow directions. Geostatistical

analyses were performed for two geologic formations and one hydrogeologic unit which may be of importance in the transport of radionuclides between the disturbed zone and the accessible environment: the Grande Ronde Formation, the Wanapum Formation and the Mabton Interbed. The geostatistical technique of kriging was used to provide interpolated values of hydaulic head elevations, as well as the uncertainty associated with each interpolated value. Interpolated hydraulic head elevations are used to construct contour maps from which groundwater flow directions are inferred.

Preliminary results showed that, in the Wanapum Formation, radionuclides can be transported northwesterly from the Reference Repository Location (RRL) toward the Columbia River, between the Umtanum-Gable Mountain anticline. In the Grande Ronde Formation, the water head elevation map did not support the DOE conceptualization of an overall southeasterly groundwater flow toward the Columbia River. More monitoring wells are needed, however, to ascertain this result.

Due to the great level of uncertainty associated with the interpolated water head elevations, groundwater directions were not interpretated in the Mabton Interbed. The failure to obtain satisfactory results suggests that the hydrogeology within this unit is too complex to be described using the existing sparse data, raising concerns about the selection of the Hanford Site as a nuclear waste repository.

High levels of uncertainty on the estimated head elevations were also observed for the Grande Ronde and Wanapum Formations. Additional monitoring wells, screened in these formations, are needed south of the RRL. East of the RRL, the Cold Creek "barrier" should also be carefully addressed by DOE. The existing data analysed could not account for such an anomaly.

A. INTRODUCTION

Under the Nuclear Waste Policy Act of 1982, the DOE has been charged with identifying the site at which the first nuclear waste repository will be constructed. The Hanford Site, located in Washington, is one of the three sites (the other two being Yucca Mountain, NV and Deaf Smith County, TX) recently recommended by the DOE and nominated by the President of the United States for site characterization. The ultimate goal of the site characterization program is to acquire site information for each of the three sites nominated to support a licensing application and the accompanying environmental impact statement.

A large scale hydraulic testing is planned as part of the site characterization program. However, prior to the hydraulic testing, the DOE must demonstrate that the existing data are sufficient to reliably predict the hydraulic baseline. The baseline in hydrologic monitoring programs, refers to the data that describe a hydrologic system prior to being disturbed or impacted. Use of the term baseline commonly assumes that (1) the baseline data should account for both spatial and temporal variability, (2) data should be adequate for use as a basis for comparison or interpretation, and (3) data should be sufficient and accurate enough for stated purposes (Sorooshian et al., 1984).

Hydraulic baseline predictions will be made using models fitted to observations obtained prior to hydraulic testing. The predicted hydraulic baseline heads along with the actual heads observed during testing will be used in the analysis to determine aquifer characteristics. These characteristics, in turn, will be used in assessing and defining the repository performance for licensing purposes. Computer modelling of the aquifer system will be intensively used in performance assessment. Interpretation of the groundwater flow system is used in developing an overall conceptualization of flow patterns and directions across the Cold Creek Syncline. This conceptualization is subsequently used to construct the models. Besides defining proper aquifer characteristics, (e.g., hydraulic conductivities, effective porosity), groundwater flow direction and adequate boundary conditions (e.g., hydraulic head gradient) must be derived from the spatial distribution of piezometric heads.

A preliminary analysis has been conducted to study the spatial distribution of piezometric data in basalt formations. The selected formations are expected to be of significance in determining the flow of groundwater and subsequent transport of radionuclides between the disturbed zone and the accessible environment. Because of the spatially discrete nature of data, the minimum variance unbiased linear estimation technique (or kriging) was used to identify the spatial distribution of water head elevations, as well as the degree of confidence of the estimated head elevations. The overall stochastic interpolation procedure is briefly outlined in Section B. Water head elevations were estimated for two geologic formations and one hydrogeologic unit of the Columbia River Basalt at the Hanford Site. The interpolation results are discussed in Section C.

B. PREDICTION OF HYDRAULIC HEAD BY LINEAR ESTIMATION

I. Linear Estimation Theory

Hydraulic heads in a defined region are estimated using minimum variance unbiased linear estimation theory or kriging. Kriging is a method for optimizing the estimation of a property which is distributed in space and sampled at a number of locations. Let $\underline{x}_1$, $\underline{x}_2$,..., $\underline{x}_n$ be the locations of the measurements and z_i the value measured at the location $\underline{x}_i$. The property z is called a regionalized variable. The problem of linear estimation lies in determining an estimate $\hat{z}_0$ of the value z_0 for any location $\underline{x}_0$. By continually modifying the position of the point $\underline{x}_0$, it is thus possible to estimate the whole field of the property z.

In the general case of linear estimation with variable drift (Matheron, 1971), the regionalized variable is given by the linear model

$$z(\underline{x}) = \underline{g}^T.\underline{b} + \varepsilon(\underline{x}) \qquad (1)$$

where $\underline{g}$ is a known vector of the spatial coordinates and $\underline{b}$ is a vector of parameters. In the case of a stationary field, $\underline{g}$ reduces to the scalar 1 and b to the mean m. In the case of a linear drift (e.g., $m(\underline{x})$ is a linear function of the vector $\underline{x}$), $\underline{g}$ is given by the vector

$$\underline{g} = \begin{bmatrix} 1 \\ x_1 \\ x_2 \end{bmatrix} \qquad (2)$$

where x_1 and x_2 are the two cartesian coordinates of location $\underline{x}$.
The estimate $\hat{z}_0$ of the value z_0 at location $\underline{x}_0$ is defined as a linear combination of the measurements

$$\hat{z}_0 = \sum_{i=1}^{n} \lambda_i . z_i \qquad (3)$$

The coefficients $\lambda_1, \lambda_2, \ldots, \lambda_n$ are selected so that the estimate is unbiased for any value of the unknown coefficients $\underline{b}$, i.e.,

$$E[\hat{z}_0] = \sum_{i=1}^{n} \lambda_i . \underline{g}_i^T . \underline{b} = \underline{g}_0^T . \underline{b} \qquad (4)$$

and the variance of estimation

$$E[(\hat{z}_0 - z_0)]^2] \qquad (5)$$

is minimum. The unbiasedness condition (4) may be rewritten

$$g_0 = \sum_{i=1}^{n} \lambda_i . g_i \qquad (6)$$

In the case of a linear drift, the universality condition (6) may be rewritten in terms of three scalar equations

$$\sum_{i=1}^{n} \lambda_i = 1 \qquad (7.a)$$

$$\sum_{i=1}^{n} \lambda_i . x_{i1} = x_{01} \qquad (7.b)$$

$$\sum_{i=1}^{n} \lambda_i . x_{i2} = x_{02} \qquad (7.c)$$

where x_{i1} and x_{i2} are the cartesian coordinates of location x_i.

If we assume that the covariance function of $z(\underline{x})$ is $R(\underline{x}_1,\underline{x}_2)$, the coefficients $\lambda_1, \lambda_2, \ldots, \lambda_n$ are estimated by solving the following minimization problem

$$\min \left\{ \sum_{i=1}^{n} \sum_{j=1}^{n} \lambda_i . \lambda_j . R(\underline{x}_i,\underline{x}_j) - 2 \sum_{i=1}^{n} \lambda_i . R(\underline{x}_i,\underline{x}_0) + R(0) \right\} \qquad (8)$$

subject to linear constraints given by the set of equations (7).

The coefficients are selected by solving the following system of n+3 equations with n+3 unknowns, $\lambda_1, \lambda_2, \ldots, \lambda_n, \nu_1, \nu_2, \nu_3$,

$$\sum_{j=1}^{n} {}_j . R(\underline{x}_i,\underline{x}_j) - \nu_1 - \nu_2\, \underline{x}_{i1} - \nu_3\, x_{i2} = R(\underline{x}_j,\underline{x}_0), \quad i=1,\ldots,n \qquad (9.a)$$

$$\sum_{i=1}^{n} \lambda_i = 1 \qquad (9.b)$$

$$\sum_{i=1}^{n} \lambda_i . x_{i1} = x_{01} \qquad (9.c)$$

$$\sum_{i=1}^{n} \lambda_i . x_{i2} = x_{02} \tag{9.d}$$

In the case of a stationary field, the terms in ν_2 and ν_3 in the n equations (9.a) drop and the kriging system reduces to the simplified set of equations (9.a) along with equation (9.b).

The variance of the error of estimation can be computed from equation (8). If one assumes that the error of estimation is normally distributed, the 95% confidence interval is $z_0 \pm 2\sigma$, σ being the standard deviation, i.e., the square root of the variance.

The linear estimation problem is therefore entirely solved once the first two moments of the stochastic field $z(\underline{x})$ are identified, e.g., a functional form for the mean and the covariance function $R(\underline{x}_1, \underline{x}_2)$ chosen.

II. Choice of a Functional Form for the Mean and the Covariance Function

A functional form of the mean and the covariance function must be selected and their parameters statistically estimated from available data. Among the possible functional models for spatially distributed fields, the class of intrinsic functions of order 0, 1 and 2 with polynomial generalized covariance functions was selected. Delfiner (1976) found that almost all sets of data that appear in practice can be satisfactorily (for purposes of interpolation) described as intrinsic functions of order 0, 1 and 2 with polynomial generalized covariance functions given by

$$R(d) = c.\delta(d) + a_1.d \tag{10.a}$$

$$R(d) = c.\delta(d) + a_1.d + a_3.d^3 \tag{10.b}$$

$$R(d) = c.\delta(d) + a_1.d + a_3.d^3 + a_5.d^5 \tag{10.c}$$

respectively, where $\delta(d)$ is Dirac's delta function, d is the separation distance between measurement locations, and c, a_1, a_3, a_5 are the unknown parameters of the polynomial generalized covariance function. $\delta(d)$ is 1 when $d=0$ and 0 in all other cases. Due to the restricted number of available data points, only intrinsic functions of order 0 and 1 were considered in this study.

III. Statistical Estimation of the Parameters

Parameter estimates are obtained by an iterative regression approach described by Kafritsas and Bras (1981). A brief review of this estimation method is given by Kitanidis (1983). In this approach, authorized linear combinations (or generalized increments) of the measurements are formed from the original data z_i,

$$z_m = \sum_{i=1}^{n} \lambda_{mi} \cdot z_i \tag{11}$$

The variance of the authorized combination z_m is estimated from the generalized covariance function R,

$$E[\, z_m^2 \,/\, \underline{\theta}] = \sum_{i=1}^{n} \sum_{j=1}^{n} \lambda_{mi} \cdot \lambda_{mj} \cdot R(\, d_{ij} \,/\, \underline{\theta}) \tag{12}$$

where $\underline{\theta}$ is the vector of parameters (e.g., c, a_1, a_3), and d_{ij}, the separation distance between the locations of measurement z_i and z_j. The parameters are estimated by minimizing the sum of squares of the differences of measured authorized combinations,

$$z_m^2 = \sum_{i=1}^{n} \sum_{j=1}^{n} \lambda_{mi} \cdot \lambda_{mj} \cdot z_i \cdot z_j \tag{13}$$

and their expected values $E[\, z_m^2 \,/\underline{\theta}]$ as defined by equation (12). That is, the criterion of performance is:

$$\min \{ \sum_{m=1}^{n} [z_m^2 - E[z_m^2 / \underline{\theta}] \} \quad (14)$$

In the iterative regression approach, first generalized increments are created using a generalized covariance function $R(d) = - d$. Coefficients are calculated by minimizing the expression (14) using these generalized increments. These coefficients are then used to create new generalized increments, and the procedure is repeated until the coefficients converge.

IV. Selection of the Best Model

The parameter estimation procedure is applied to all possible models described by equations (10.a) and (10.b). There are ten possible models which are described by

$$\begin{aligned} R(d) &= c.\ \delta(d) \\ R(d) &= a_1.d \\ R(d) &= c.\ \delta(d) + a_1.d \end{aligned} \quad (15)$$

for the intrinsic field of order 0, and by

$$\begin{aligned} R(d) &= c.\ \delta(d) \\ R(d) &= a_1.d \\ R(d) &= a_3.d^3 \\ R(d) &= c.\ \delta(d) + a_1.d \\ R(d) &= c.\ \delta(d) + a_3.d^3 \\ R(d) &= a_1.d + a_3.d^3 \\ R(d) &= c.\ \delta(d) + a_1.d + a_3.d^3 \end{aligned} \quad (16)$$

for the intrinsic field of order 1. The parameters for each of the ten models are estimated using the procedure outlined previously. The models that are proper (i.e., conditionally positive definite) generalized covariance functions are compared to select the best one. The best model is obtained through a ranking procedure (Kafritsas and Bras, 1981): the models are used to estimate values of z at points where z values are available; they are then ranked according to their error of estimation at each data point (1 for the best, 2 for the second best, etc); the ranks are averaged over the total number of data points; the best model is the one that has the lowest average rank.

C. HEAD ELEVATION ESTIMATION FOR THREE BASALT FORMATIONS

Two geologic formations and one hydrogeologic unit of the Columbia River Basalt at the Hanford Site were selected for this study: The Wanapum Formation, the Grande Ronde Formation, and the Mabton Interbed. The selection was based on the potentiality of these formations to act as discharge zones for the groundwater system under the operating conditions of the repository. Selection of the whole geologic formation (e.g., Wanapum and Grande Ronde) instead of selected hydrogeologic units has been dictated by the insufficient number of observations available for each hydrogeologic unit within these formations. The linear estimation technique is used to estimate hydraulic heads. Structural models of the hydraulic head field are identified and subsequently used in the kriging system. Hydraulic head estimates are obtained at each node of a grid that overlays the southern part of the Hanford Site boundaries (Figure 1).

I. Description of the Data Used

Rockwell Hanford Operations is monitoring water levels at three piezometer cluster sites at the RRL and at 35 additional boreholes at the Hanford Site (Figure 1). The water-level information is being used to evaluate time variant hydraulic head behavior and to establish a head baseline for selected hydrogeologic units.

The water level data for the three piezometer cluster sites, DC-19, DC-20 and DC-22, used in this analysis were taken from a data package published by the DOE (Bryce and Yeatman, 1984). The water level data for the 35 Basalt Waste Isolation Project (BWIP) monitoring wells were provided in a data package prepared by Swanson and Wilcox (1985).

The monitoring boreholes are screened ~~in~~ several hydrogeologic units in the Columbia River Basalts. In order to have enough water level observations to apply the geostatistical approach described earlier, the boreholes that are screened in different members of the Wanapum and Grande Ronde geological formations were grouped together. Since the screens of some boreholes intersect more than one member in the same formation, classification of these boreholes in terms of the whole formation seems justified. In the Grande Ronde Formation, only boreholes screened in the upper members (i.e., Sentinel Bluffs Sequence) were considered. The classification led to three groups of boreholes which were screened in the Mabton Interbed and the Wanapum and the Grande Ronde basalts, respectively (Table 1). The water levels used in the analysis were measured from October 1, 1984 to October 5, 1984. The borehole locations and the water level measurements are presented in Tables 2 through 4.

II. Estimation of Hydraulic Heads

1. Wanapum Formation

a. Identification of a structural model

Sixteen boreholes are monitored in the Wanapum Formation (Table 1). Most of the boreholes are screened in the Priest Rapids member. During the period of interest, only thirteen water level measurements were available (Table 3). Among these 13 observations, the water levels observed at Ford and O'Brian wells were 500 feet higher than those in the rest of the boreholes. The hydraulic heads in the upper Wanapum Basalt of the Cold Creek Valley are

Table 1: Borehole Distribution

Mabton Interbed	Wanapum	Grande Ronde
DB-4	DB-1	DC-2
DB-7	DB-2	DC-4/5
DB-9	DB-12	DC-7/8
DB-13	DB-14	DC-12
DC-16	DB-15	DC-15
DC-19	DC-1	RRL-2A
DC-20	DC-16C	RRL-6B
DC-22	DC-19	RRL-14
	DC-20	DC-19
	DC-22	DC-20
	DDH-3	DC-22
	ENYEART	
	FORD	
	O'BRIAN	
	DB-11	
	McGEE	

Table 2: Water level measurement in the Mabton Interbed on the 1 through 5 October, 1984.

Borehole#	Location North	Location East	Water level (feet)
DB-4	439,903	2,267,800	418.30
DB-7	388,963	2,271,833	400.59
DB-9	467,360	2,238,509	403.88
DB-13	422,511	2,247,964	420.46
DC-16	436,353	2,211,520	420.75
DC-19	433,849	2,225,136	420.84
DC-20	452,008	2,215,170	414.04
DC-22	448,530	2,204,074	410.59

Table 3: Water level measurement in the Wanapum on the 1 through 5 October, 1984.

Borehole#	Location North	East	Water level (feet)
DB-1	406,971	2,308,893	392.8
DB-2	420,657	2,308,000	394.2
DB-12	468,067	2,200,144	397.4
DB-14	430,190	2,215,764	400.1
DB-15	452,503	2,253,430	404.7
DC-1	453,178	2,247,000	403.8
DC-16	436,377	2,211,009	401.9
DC-19	433,933	2,225,012	399.8
DC-20	451,884	2,215,288	401.4
DC-22	448.600	2,204,188	400.4
DDH-3	374,957	2,304,900	391.1
ENYEART	454,397	2,183,844	908.19*
FORD	458.009	2,183,788	912.34
O'BRIAN	457,656	2,181,139	912.05
DB-11	454471	2,194,850	----
McGEE	457,773	2,191,775	----

* observed on October 17,1984.

Table 4: Water level measurement in the Grande Ronde on the 1 through 5 October, 1984.

Borehole#	Location North	East	Water level * (feet)
DC-2A2	453,144	2,246,946	409.43
DC-4	454,467	2,209,995	422.69
DC-7/8	420,175	2,280,448	402.14
DC-12	415,290	2,241,612	401.39
DC-15	389,808	2,309,775	401.54
RRL-2A	444,298	2,211,184	401.83
RRL-6B	438,580	2,206,413	401.39
RRL-14	446,541	2,203,992	-
DC-19	433,933	2,225,012	400.80**
DC-20	451,884	2,215,288	402.21**
DC-22	448,600	2,204,188	401.90**

* All water level data are taken from Swanson and Wilcox (1985), except for the borehole clusters DC-19, DC-20, and DC-22 for which data were taken from Yeatman and Bryce (1984).

** These water levels are an average of the water elevations observed in the Rocky Coulee Flow Top and in the Cohassett Flow Top.

generally higher than the head elevations in the same stratigraphic horizon within the RRL east of the Cold Creek "Barrier" (Figure 2). This anomaly is interpreted by DOE as a no-flow or low-flow lateral boundary (DOE, 1986). However, this interpretation has not yet been substantiated by sufficient evidence. Since the water levels at the Ford and O'Brian wells behave differently than those at the other wells, and since such anomalies cannot be accounted for by a covariance function derived from a limited number of observations, these observations were dropped in the model identification procedure.

As shown on Figure 1, most of the boreholes screened in the Wanapum Formation are located in the vicinity of the RRL. Only DB-1, DB-2 and DDH-3 are located in the southeastern part of the Hanford Site. The effect of incorporationg these three boreholes in the analysis on the estimated hydraulic head has been investigated. Structural models have been identified in two cases: (1) using observations from all eleven boreholes, and (2) not accounting for observations at boreholes DB-1, DB-2, and DDH-3.

b. Prediction of hydraulic head using eight measurements

The identification of a model has been performed using the procedure outlined previously. Only observations from boreholes DB-12, DB-14, DB-15, DC-1, DC-16, DC-19, DC-20, and DC-22 were used. Due to the paucity of data, it was not possible to select with sufficient confidence a single polynomial generalized covariance function as best describing the spatial structure of the hydraulic heads. Two models were therefore ranked equally in the ranking procedure: an intrinsic function of order 0 with polynomial covariance function given by

$$R(d) = -0.264\ d, \qquad \text{(Model 1)}$$

and an intrinsic function of order 1 with generalized covariance function

$$R(d) = -0.241\ d. \qquad \text{(Model 2)}$$

These two models were used to estimate, using point kriging, the hydraulic heads over a domain that overlays the southern part of the Hanford Site boundaries. Kriging also provided the variance of estimation error. The maps of hydraulic head estimates and variances of estimation error for the first and second models are shown in Figures 3, 4 and 5, 6, respectively. The results from both models show an overall groundwater flow in a southwestward direction (Figures 3 and 5). These kriging results, based only on information from eight boreholes, do not support the DOE interpretation of a southeasterly regional groundwater movement. It should be noted that due to the high variance of hydraulic head estimates, the model predictions in the southeastern portion of the Hanford Site boundaries is unreliable.

At the RRL, the models indicate a groundwater flow direction to the northwest. This change in flow direction agrees with part of the DOE (1982) interpretation of the groundwater movement: "Because the existence of a hydraulic low near the Umtanum Ridge-Gable Mountain anticline, shallow groundwater from the northern portion of the RRL may flow north rather than east to southeast...".

c. Prediction of hydraulic heads using eleven measurements

The observed water levels at boreholes DB-1, DB-2, and DDH-3 have been used in conjunction with the information from the above eight boreholes. The identification procedure was applied using this set of 11 data points. The best model that described the spatial structure of hydraulic head is an intrinsic function of order 0 with generalized covariance function given by

$$R(d) = -0.201\ d. \qquad \text{(Model 3)}$$

The identified generalized covariance function was used to obtain estimates of hydraulic heads, as well as variance of estimates, in a domain overlying the southern portion of the Hanford Site boundaries. The maps of predicted heads and variance of estimation error are shown in Figures 7 and 8, respectively. The comparison between the potentiometric maps shown in Figures 3, 5, and 7 lead to some remarks: (1) All three models predict a northwestward groundwater flow in the northern portion of the RRL, and (2) the differences in groundwater flow direction occur in the eastern portion of the Hanford Site boundaries; on Figure 7, the groundwater is shown to flow southeasterly between DB-15 and DB-2.

In the eastern portion of the RRL, the groundwater flow direction is not well defined. The three models predicted a southeastern to southwestern local groundwater flow direction. The presence of a groundwater flow divide in the RRL vcinity induces a certain amount of uncertainty in directional gradient estimates. The DOE used observed water levels at DC-19, DC-20 and DC-22 to estimate the directional gradients (DOE, 1986, Sorooshian et al., 1985). Borehole clusters DC-19, DC-20, and DC-22, however, may not be adequately located to provide accurate estimates of directional gradients. DC-22 is located downgradient of the groundwater flowing north; whereas DC-19 is located downgradient of the groundwater flowing south. As a result, hydraulic gradients calculated using observations from these three monitored boreholes may be underestimated. The actual hydraulic gradients of the groundwater flowing north and south in and near the RRL are probably more important.

2. Grande Ronde Formation

a. Identification of a structural model

Eleven boreholes are screened in the Grande Ronde Formation (Table 1). Only 10 of the 11 boreholes had been monitored during the period of interest.

No data is available for borehole RRL-14. In addition, the water elevation observed at borehole DC-4 is too high compared to those observed at neighboring boreholes DC-20 and DC-22. This measurement has been dropped and only the nine remaining observed water elevations have been used in the structural model identification procedure.

b. Prediction of hydraulic heads

Again, due to the paucity of the data observations, two structural models were identified: an intrinsic field of order 0 with generalized covariance function

$$R(d) = -0.359\ d, \qquad \text{(Model 1)}$$

and an intrinsic field of order 1 that assumes a linear southwestern drift, with generalized covariance function

$$R(d) = -0.335\ d. \qquad \text{(Model 2)}$$

Using point kriging, these two covariance functions were used to estimate the water head elevation over a domain overlying the southern portion of the Hanford Site boundaries.

The maps of water heads and variance of estimation errors are shown in Figures 9 and 10 for the first model and in Figures 11 and 12 for the second model. The kriged hydraulic head estimates obtained from the two models are again very consistent in the northwestern part of the model domain. The maps of variance shows that the estimation error is the smallest in this region. This result was expected since most of the monitoring boreholes are concentrated in this region. Contrary to what was found in the Wanapum Formation, no northwesterly groundwater movement is shown to occur near the RRL. Both models indicate a southwesterly groundwater flow in the vicinity of the RRL. It should be noted, however, that in the case of the Wanapum, the head elevation was observed at DB-12 which is located on the northwestern portion of the domain, whereas in the case of the Grande Ronde Formation, no such observation is available. According to the DOE 1986, an examination of hydraulic head distribution near the Umtanum Ridge-Gable Mountain anticline and between the northern border of the RRL and the Columbia River is planned. These future observations will be very helpful in the understanding of the groundwater flow movement, north of the RRL.

The two models predicted an overall southwesterly groundwater flow movement. However, this regional groundwater direction may be accurate only in the northwestern portion. Due to the high variance of the estimation error, the heads in the northeastern and the southeastern part of the domain are predicted with ± 8 to ± 11 feet uncertainty for a 95% interval of confidence (Figure 10 and 12). These last values along with the low differences in hydraulic head (of approximately 1 foot) observed at boreholes DC-7/8, DC-12 and DC-15 demonstrate the limitations of predicting a groundwater flow direction based on observed hydraulic head at only a few locations.

3. Mabton Interbed

a. Identification of a structural model

Eight boreholes are screened in the Mabton Interbed hydrogeologic unit (Table 1). Most of these boreholes are located in the vicinity of the RRL. Only borehole DB-7 is located in the southeastern portion of the Hanford Site boundaries. The identification procedure described earlier has been applied to this set of data.

b. Prediction of hydraulic head

The hydraulic head field seems to be described by an intrinsic function of order 0 with polynomial generalized covariance function

$$R(d) = -3.239\ d.$$

The head elevations obtained by using this generalized covariance function are far from satisfactory. The predicted water elevation and estimation error maps are shown on Figures 13 and 14, respectively. The variances of estimation errors are much higher than those calculated for the Wanapum and Grande Ronde Formations. The 95% confidence interval is at least ± 14 feet over the whole domain. In the case of the Mabton Interbed, the potentiometric map is very uncertain; therefore, no tentative interpretation has been made. However, the difficulty in matching a model that can predict the potentiometric map with a reasonable degree of confidence may be a sign of a more complicated groundwater flow movement in the Mabton Interbed.

D. CONCLUSION

The BWIP site at Hanford, Washington, has been selected for site characterization to determine its suitability for deep geologic nuclear waste disposal. A preliminary analysis of available water level data was made for two geologic formations and one hydrogeologic unit of the Columbia River Basalt at Hanford Site: the Wanapum Formation, the Grande Ronde Formation and the Mabton Interbed.

Kriging was employed to interpolate water head elevations and estimate associated levels of confidence. From the interpolated map of water head elevations, groundwater flow directions are inferred for the Wanapum and Grande Ronde Formations. For the Mabton Interbed, no interpretation of groundwater flow direction was attempted because of the great amount of uncertainty associated with interpolated values. The DOE believes that the overall deep groundwater flow direction for the Cold Creek Syncline is southeast along the synclinal axis. The regional southeasterly groundwater flow direction in the Wanapum Formation was confirmed by the interpolated potentiometric map only when the observations at the boreholes DB-2, DB-1 and DDH-3, which are located in the southeastern portion of the Hanford Site boundaries, were used in the interpolation prodedure. In the Grande Ronde Formation, the interpolated potentiometric map showed a south to southwesterly groundwater flow movement. However, a great amount of uncertainty was associated with the water head estimates over major part of the modeled domain. Despite this level of uncertainty, it is believed that the groundwater movement is more complicated than simply a southeasterly groundwater flow along the Cold Creek Syncline axis as believed by DOE 1986.

In order to develop a reliable overall conceptualization of flow patterns and directions across the Cold Creek Syncline more monitoring boreholes are needed. New boreholes are needed not only east of the RRL along the structural trend of the Cold Creek Syncline axis but also northeast of the RRL to investigate the potential for the discharge toward the Columbia River, between the Umtanum Ridge and Gable Mountain.

Boreholes screened in the Grande Ronde Formation are also needed south of the RRL in order to develop a better understanding of the groundwater movement in this geologic formation.

Finally, the anomaly referred to by the DOE as the Cold Creek hydrologic "barrier" has not been addressed in this study. Understanding the nature of the Upper Cold Creek Syncline anomaly is important due to its potential for affecting the present and future groundwater flow regime in the RRL.

REFERENCES

Bryce, R. W., and R. A. Yeatman, 1986, Water Level, Downhole Pressure and Atmospheric Pressure Measurements from Piezometer Clusters DC-19, DC-20, and DC-22, October 1 through October 31, 1986, SD-BWI-DP-056, Rockwell Hanford Operations, Richland, Washington.

Delfiner, P., 1976, Linear Estimation of Nonstationary Spatial Phenomena, in: Advance Geostatistics in the Mining Industry, edited by M. Guarascio, M. David, and C. Huijbregts, pp 49-68, D., Reidel Publishing Co., Boston.

Department of Energy, 1982, Site Characterization Report for the Basalt Waste Isolation Project, DOE/RL 82-3, 3 Vols., Rockwell Hanford Operations for the U.S. Department of Energy, Washington, D.C.

Department of Energy, 1986, Environmental Assessment, Reference Repository Location, Hanford Site, Washington, DOE/RW-0070, 3 Vols., U.S. Department of Energy, Office of Civilian Radioactive Waste

Kafritsas, J., and R. L. Bras, 1981, The Practice of Kriging, Tech. Rep. 263, 107 pp., Ralph M. Parsons Lab., Mass. Inst. of Technol., Cambridge.

Kitanidis, P. K., 1983, Statistical Estimation of Polynomial Generalized Covariance Functions and Hydrologic Applications, Water Resources Research, Vol. 19, No. 4, Pages 909-921.

Matheron, G., 1971, The Theory of Regionalized Variables and its Applications, 212 pp., Ecole des Mines, Fontainebléau, France.

Sorooshian, S., D. R. Davis, L. K. Kher, and T. C. Rasmussen, 1984, Criteria for Baselining of Time-Variant Hydrologic Parameters, BWIP Service Agreement SA-1008.

Sorooshian, S., D. R. Davis, T. C. Rasmussen, and R. H. Nevulis, 1985, Baseline Prediction Models, Baseline Prediction Model Validation, Ground-water Level Correlations, Direction and Magnitude of Ground-water Gradients, and Optimal Sampling Frequencies, BWIP Service Agreement SA-6034.

Swanson, L. C., and S. E. Wilcox, 1985, Water-Level Data Monitoring Wells Used by the Basalt Waste Isolation Project from October 1, 1984 through March 31, 1985, SD-BWI-DP-064, Rockwell Hanford Operations, Richland, Washington.

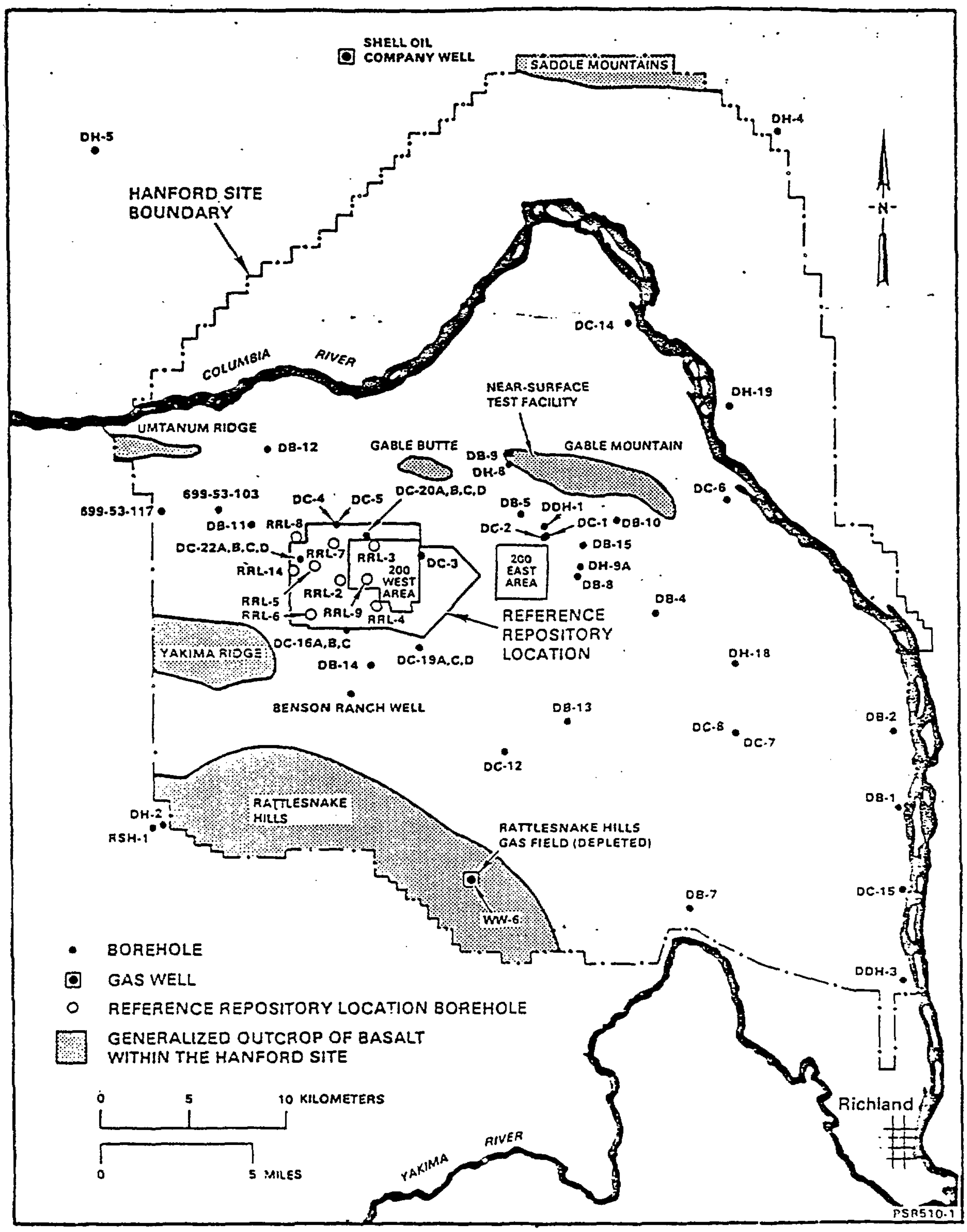

FIGURE 1: LOCATION MAP FOR SELECTED BOREHOLES

EWA

ENGINEERING FOR EARTH • WATER • AIR RESOURCES

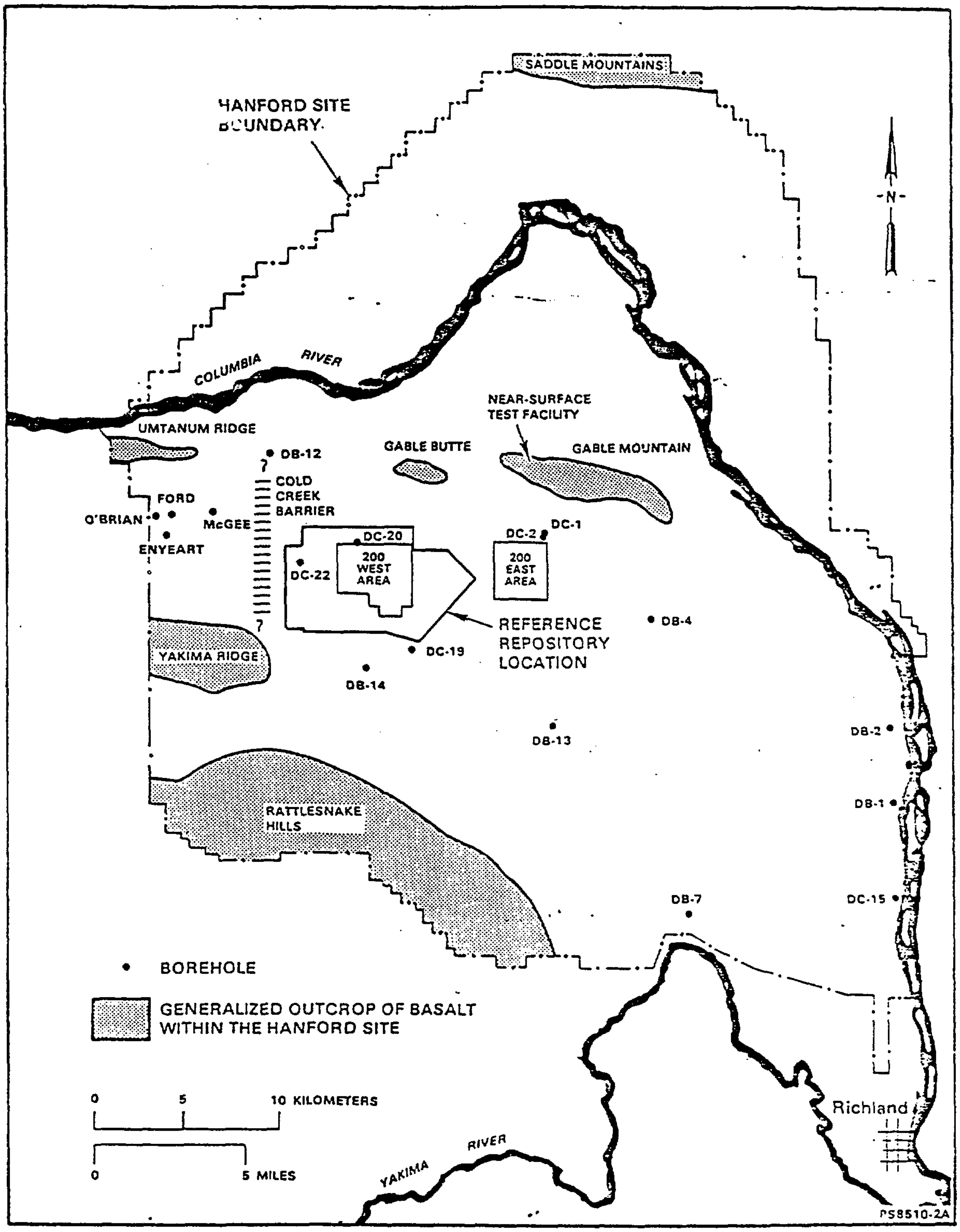

FIGURE 2: LOCATION MAP FOR SELECTED BOREHOLES

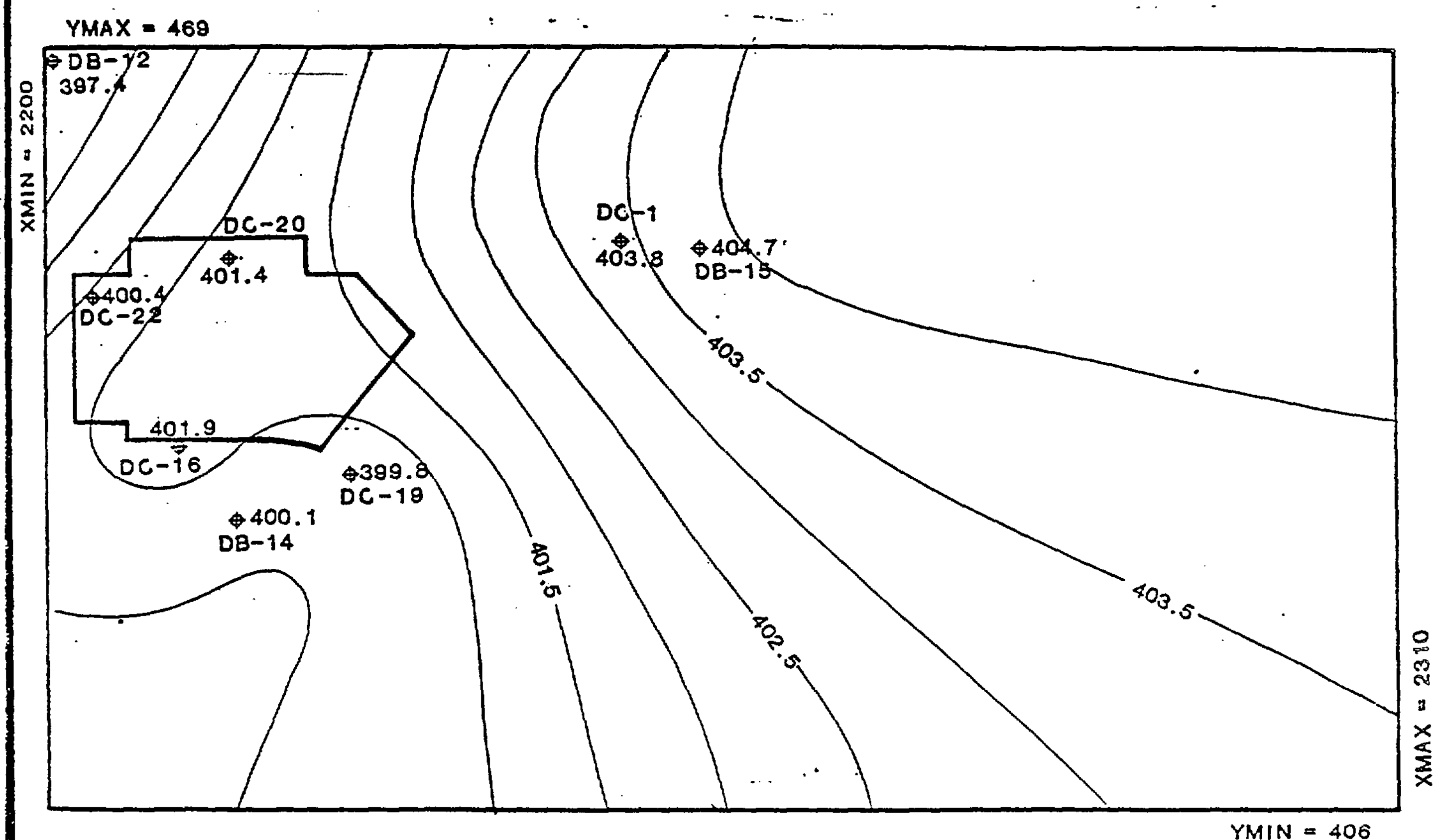

FIGURE 3: WANAPUM (MODEL 1)

MAP OF HEAD ELEVATIONS

ENGINEERING FOR EARTH • WATER • AIR RESOURCES

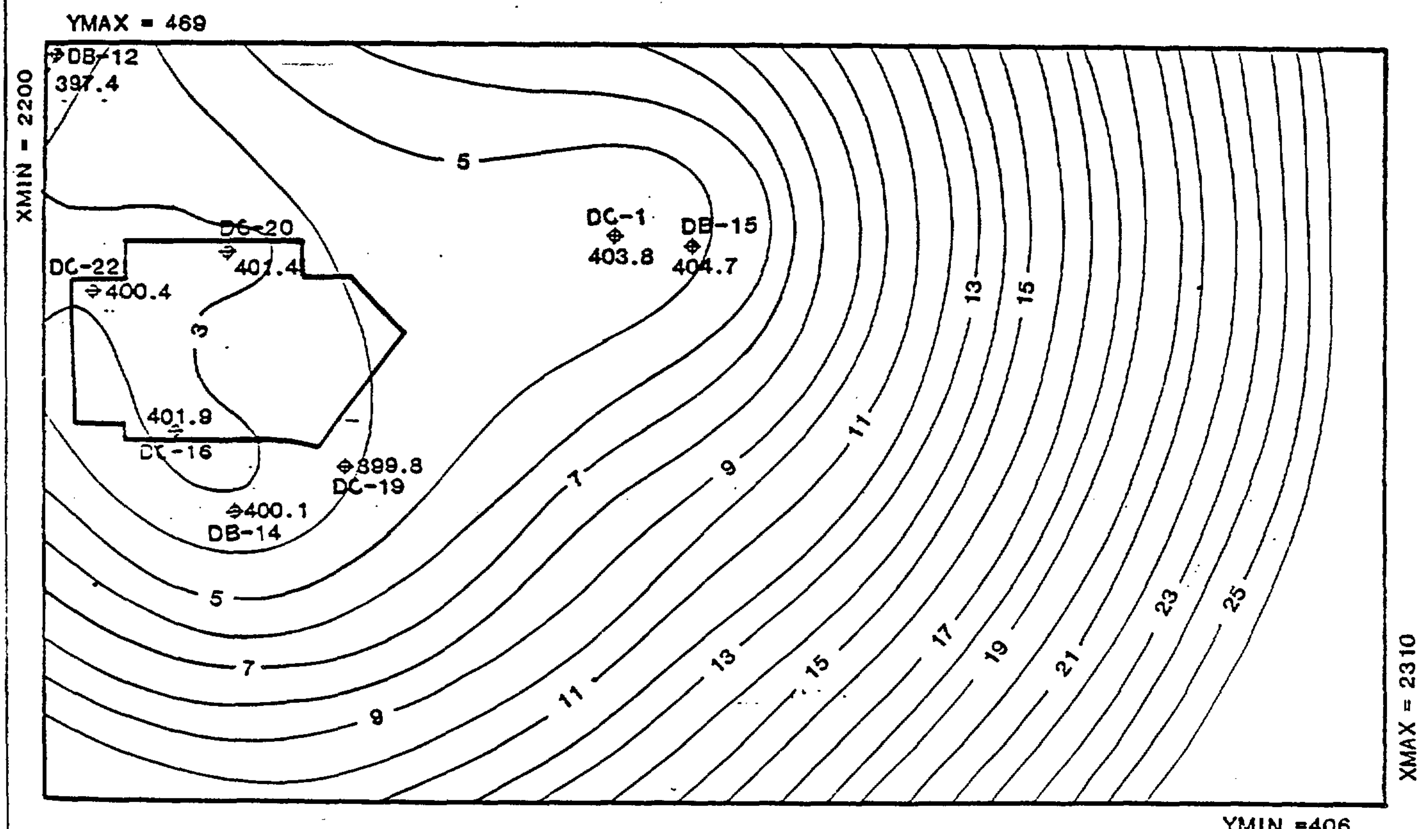

FIGURE 4: WANAPUM (MODEL 1)
VARIANCE OF ESTIMATION ERROR

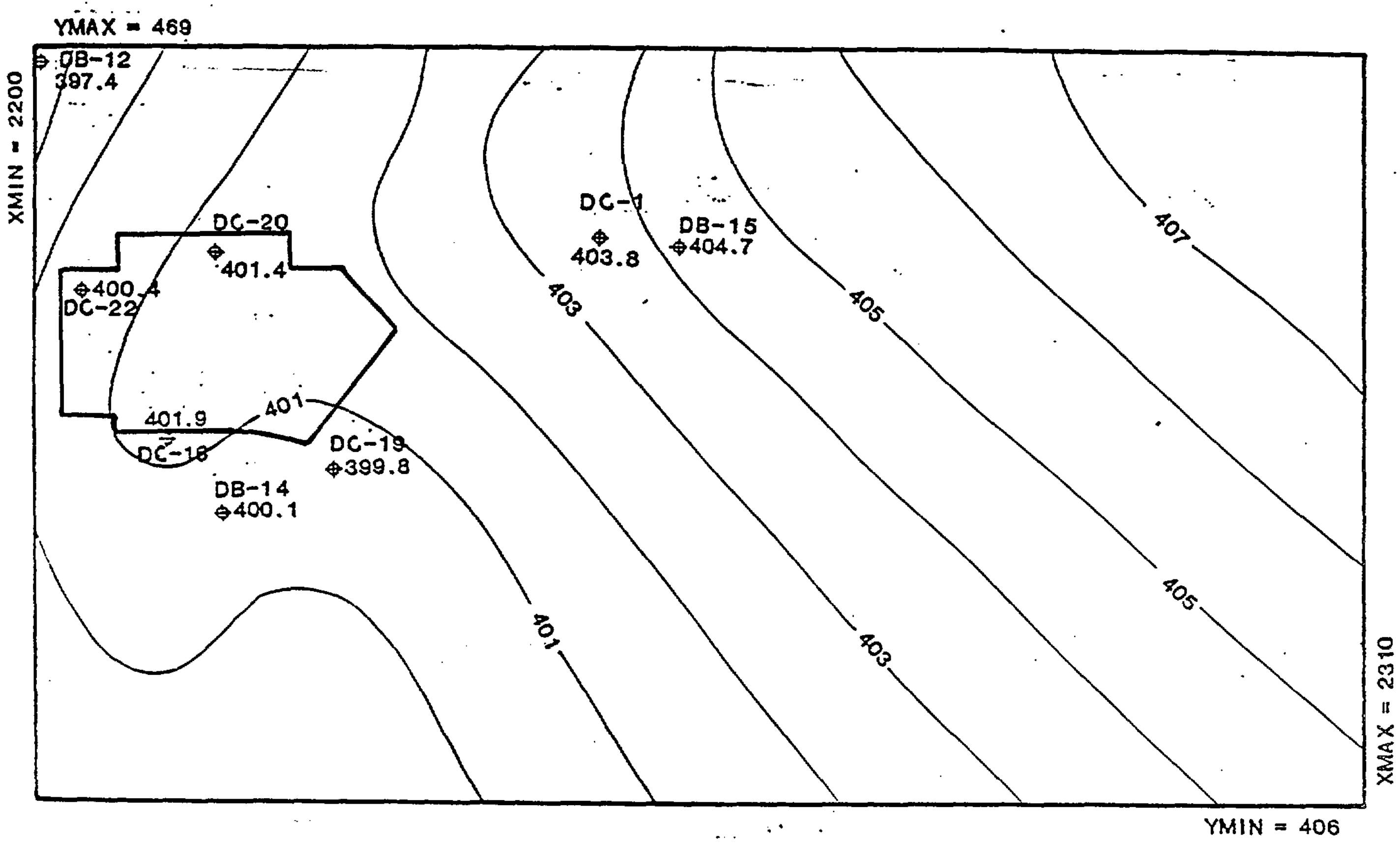

FIGURE 5: WANAPUM (MODEL 2)
MAP OF HEAD ELEVATIONS

ENGINEERING FOR EARTH • WATER • AIR RESOURCES

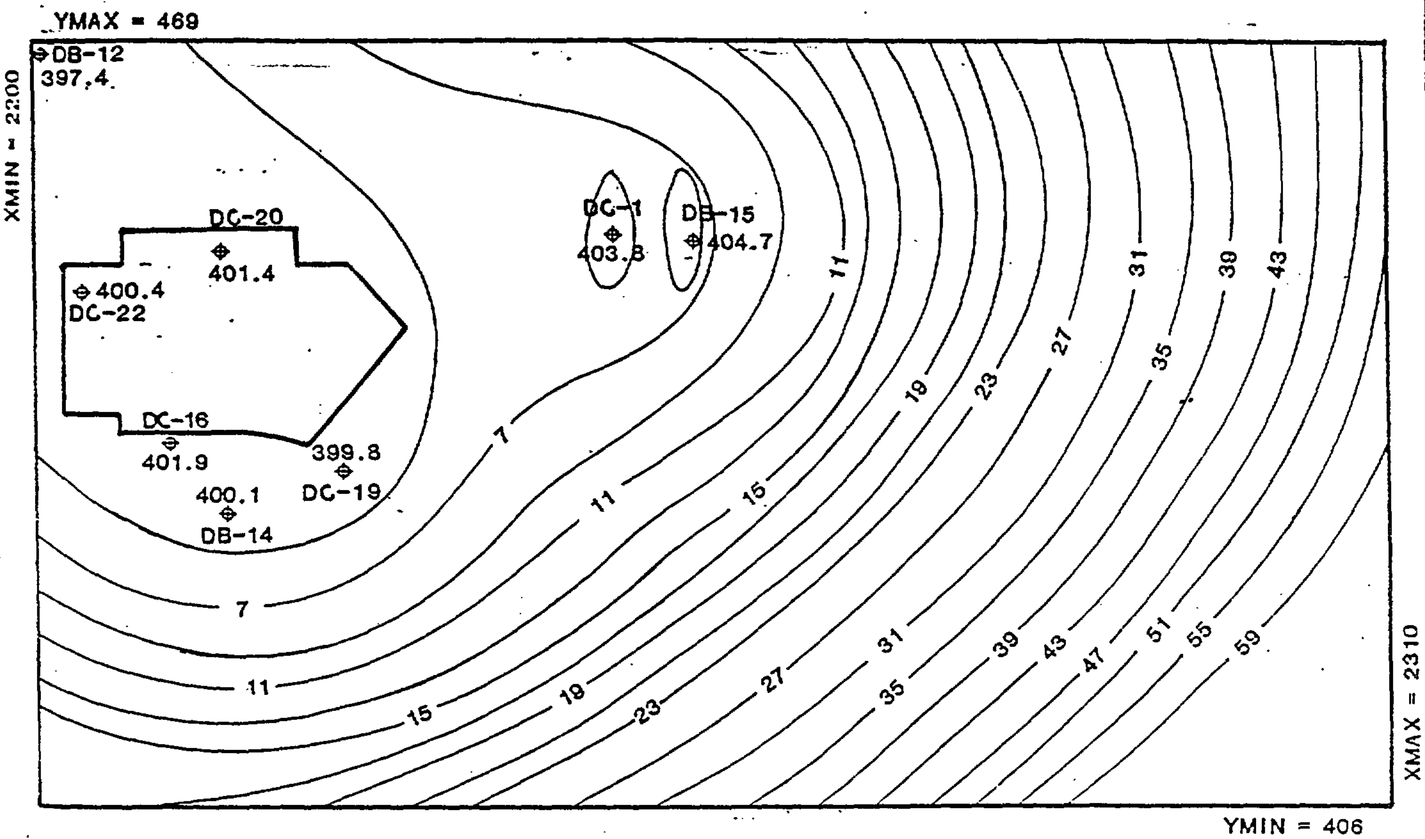

FIGURE 6: WANAPUM (MODEL 2)
VARIANCE OF ESTIMATION ERROR

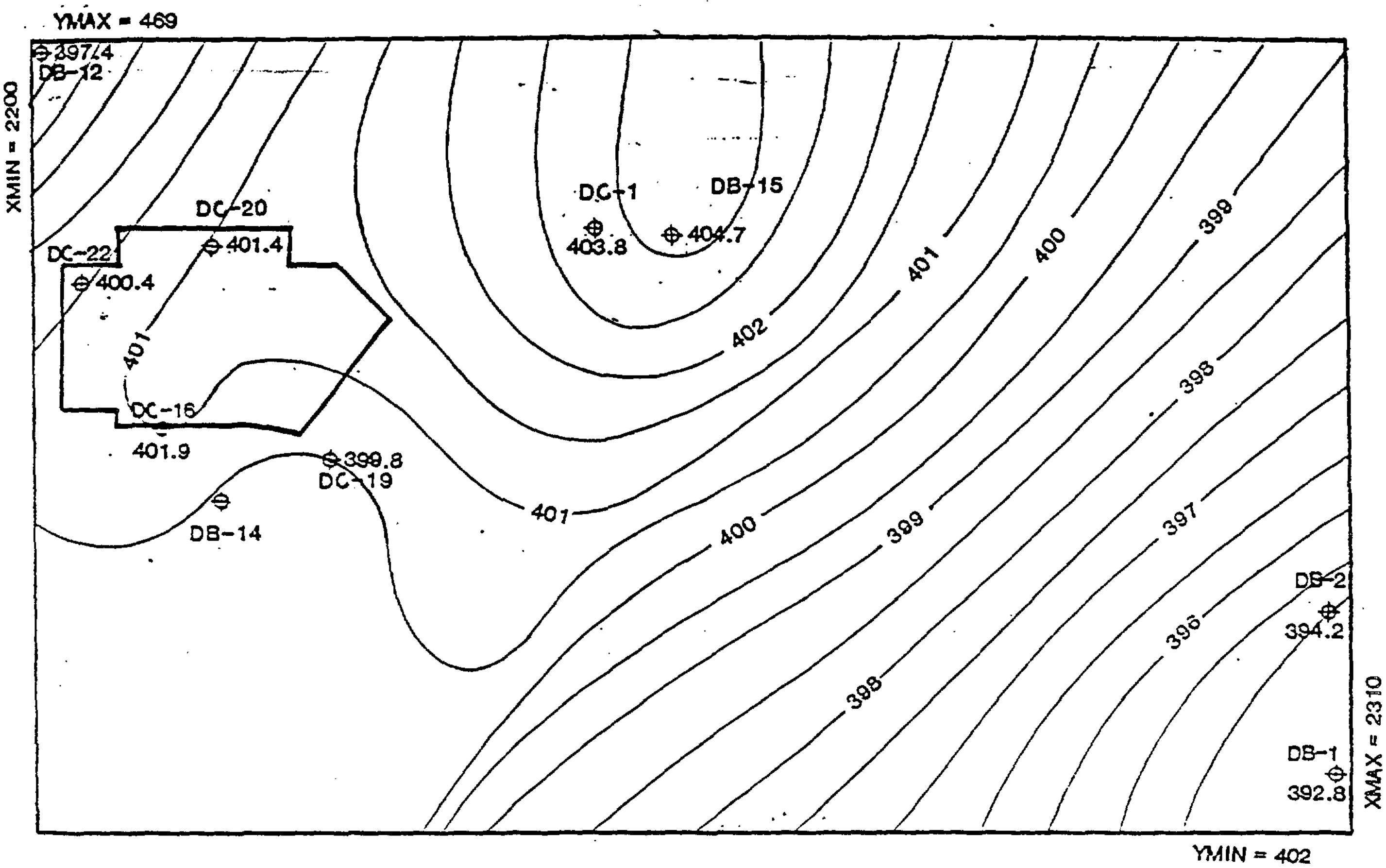

FIGURE 7: WANAPUM (MODEL 3)
MAP OF HEAD ELEVATIONS

ENGINEERING FOR EARTH • WATER • AIR RESOURCES

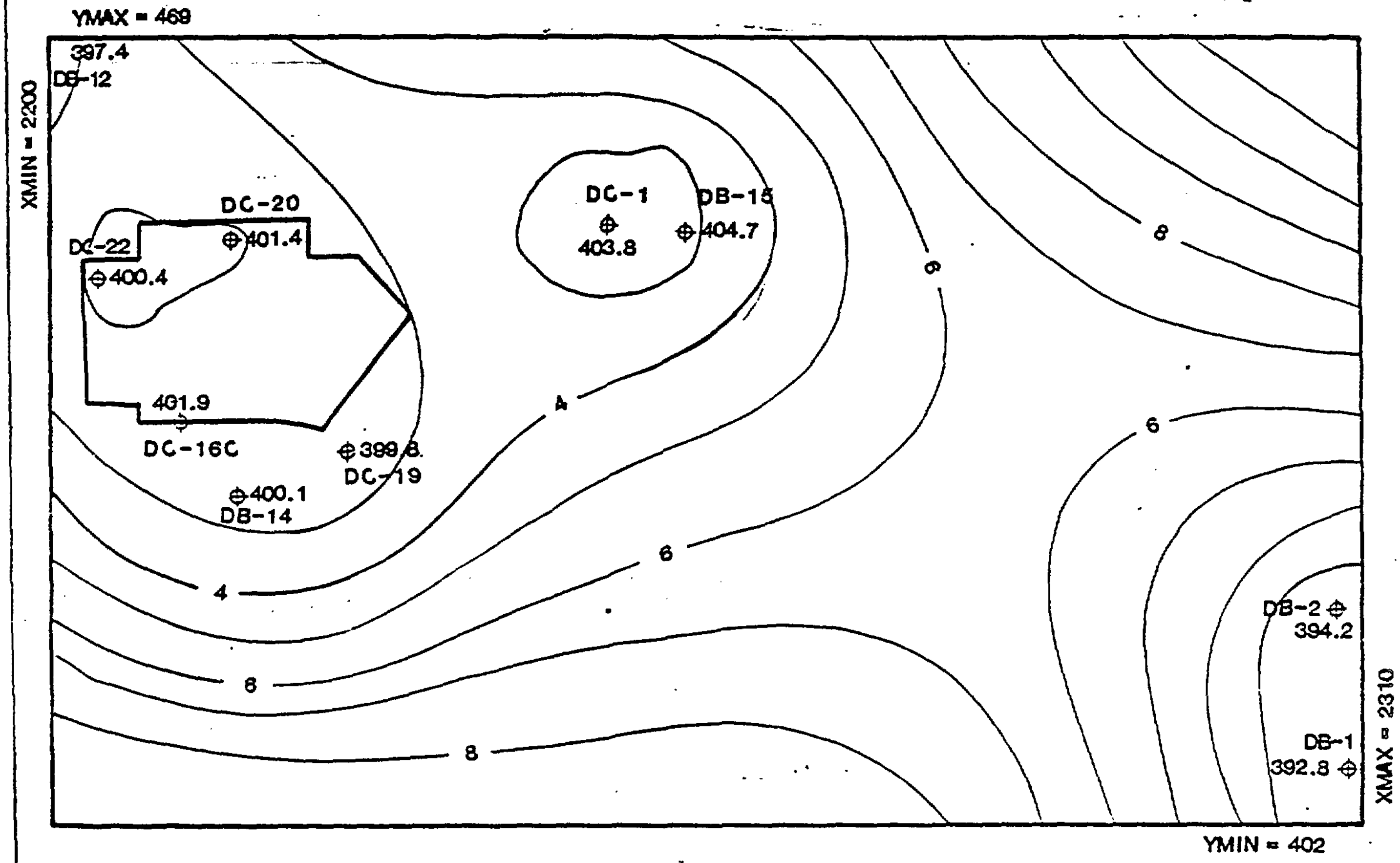

FIGURE 8: WANAPUM (MODEL 3)
VARIANCE OF ESTIMATION ERROR

ENGINEERING FOR EARTH • WATER • AIR RESOURCES

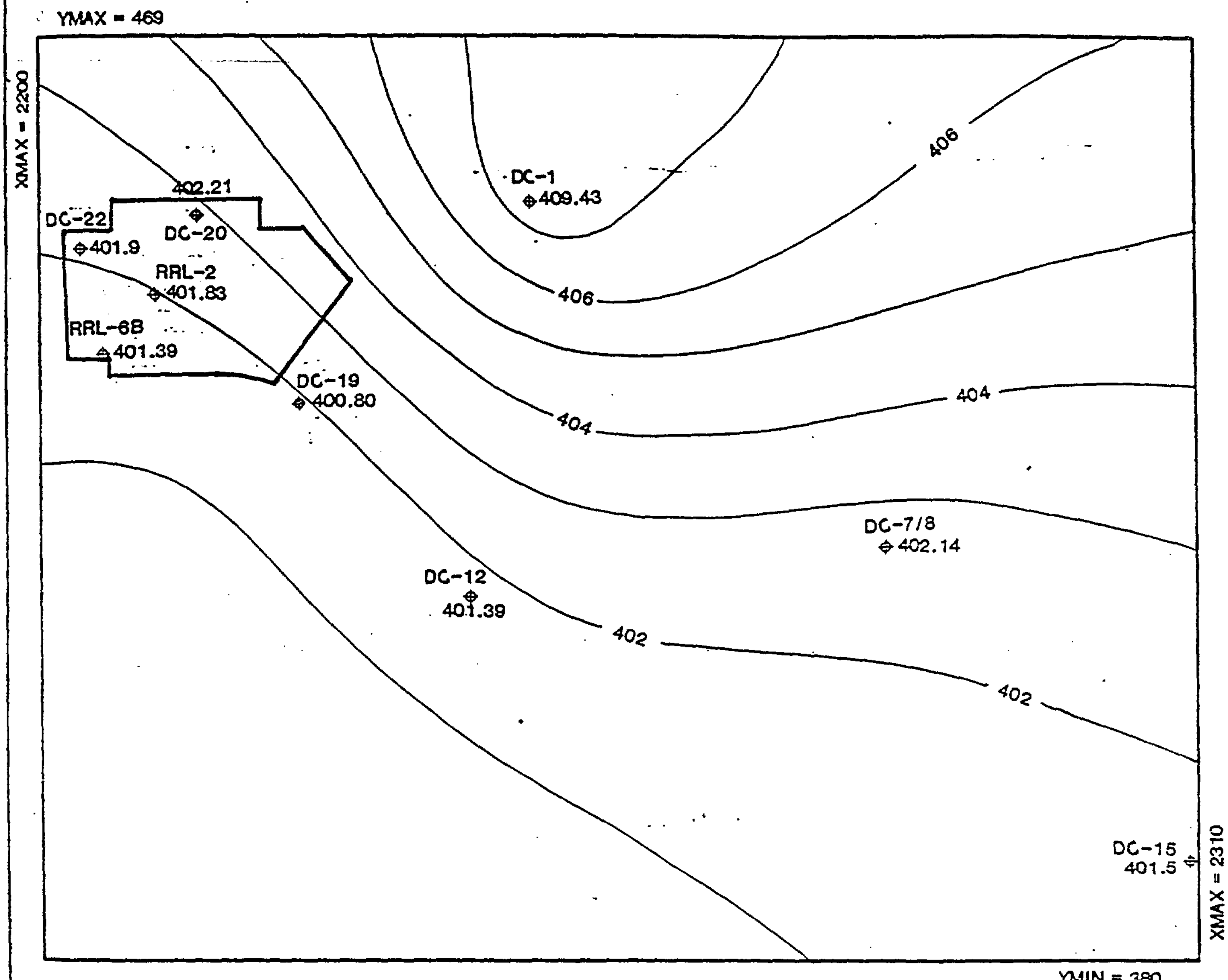

FIGURE 9: GRANDE RONDE (MODEL 1)
MAP OF HEAD ELEVATIONS

ENGINEERING FOR EARTH • WATER • AIR RESOURCES

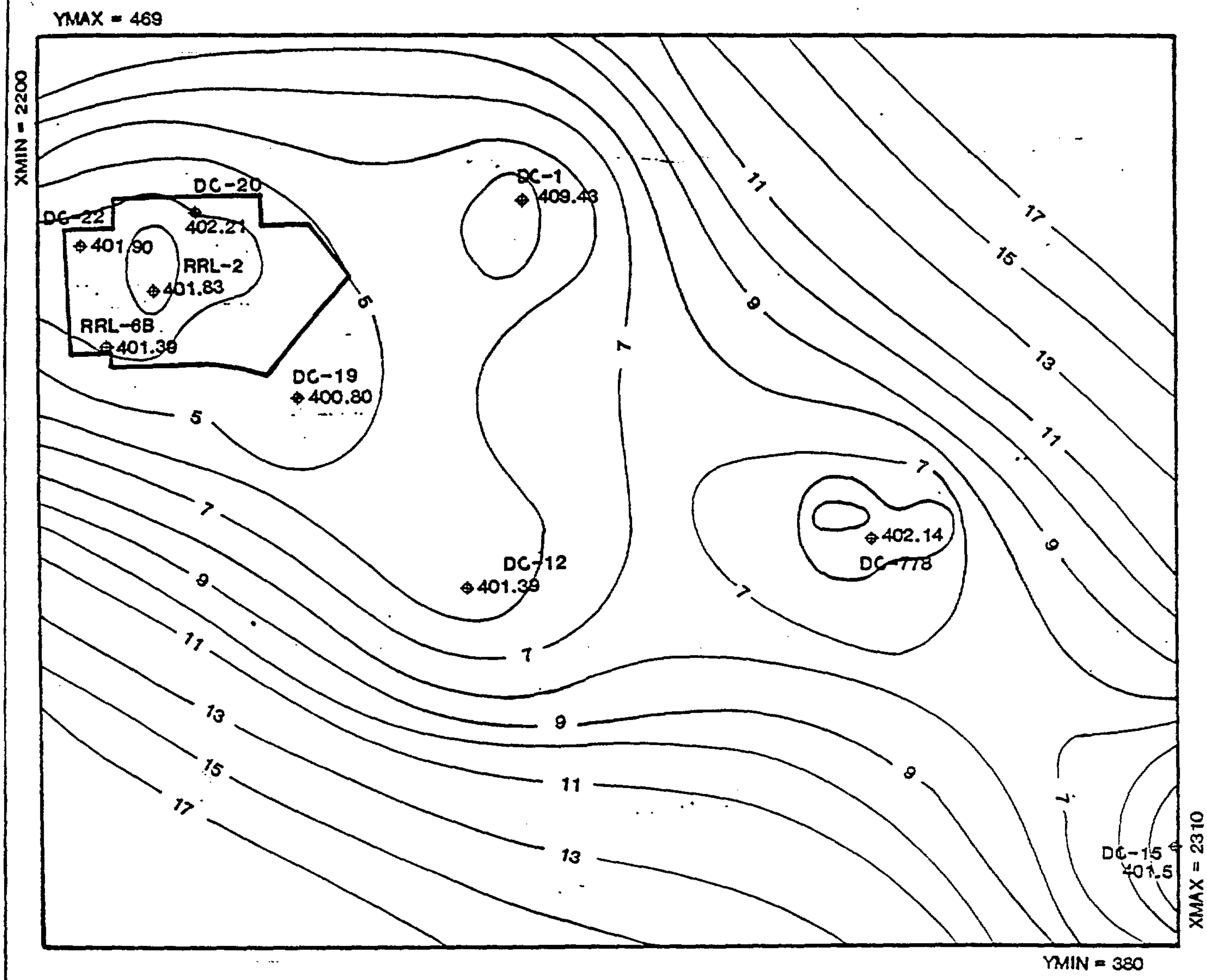

FIGURE 10: GRANDE RONDE (MODEL 1)
VARIANCE OF ESTIMATION ERROR

ENGINEERING FOR EARTH • WATER • AIR RESOURCES

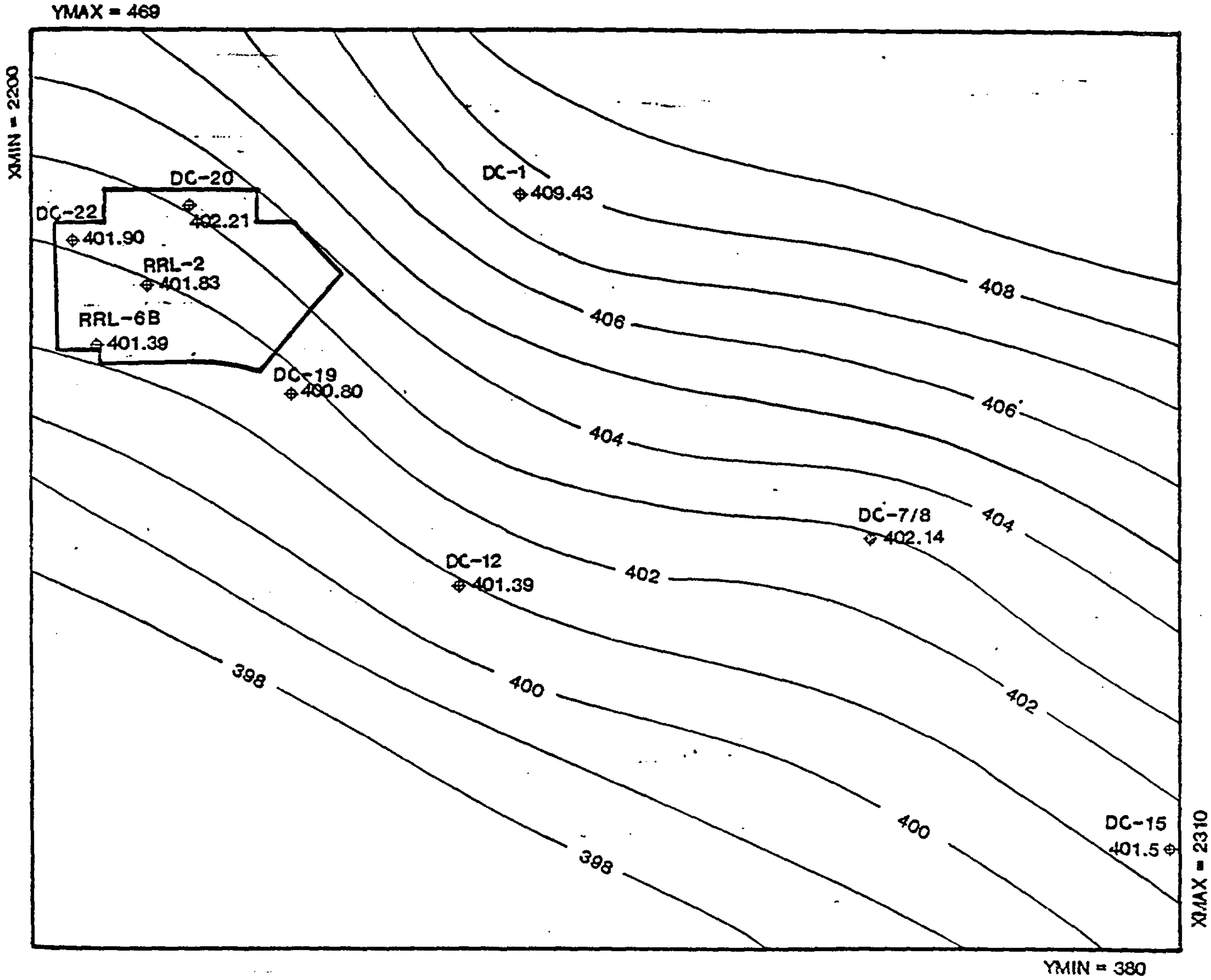

FIGURE 11: GRANDE RONDE (MODEL 2)
MAP OF HEAD ELEVATIONS

ENGINEERING FOR EARTH • WATER • AIR RESOURCES

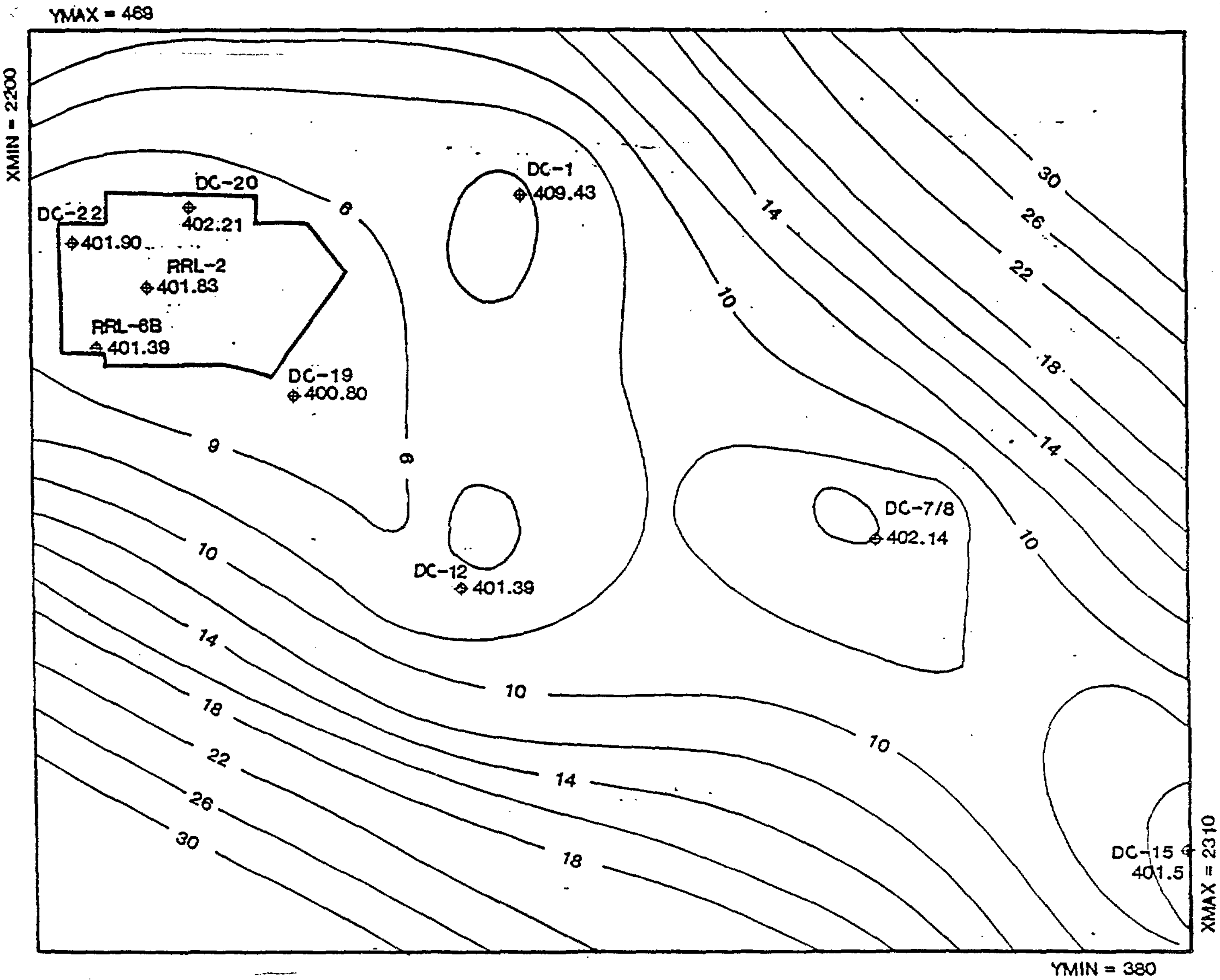

FIGURE 12: GRANDE RONDE (MODEL 2)
VARIANCE OF ESTIMATION ERROR

ENGINEERING FOR EARTH • WATER • AIR RESOURCES

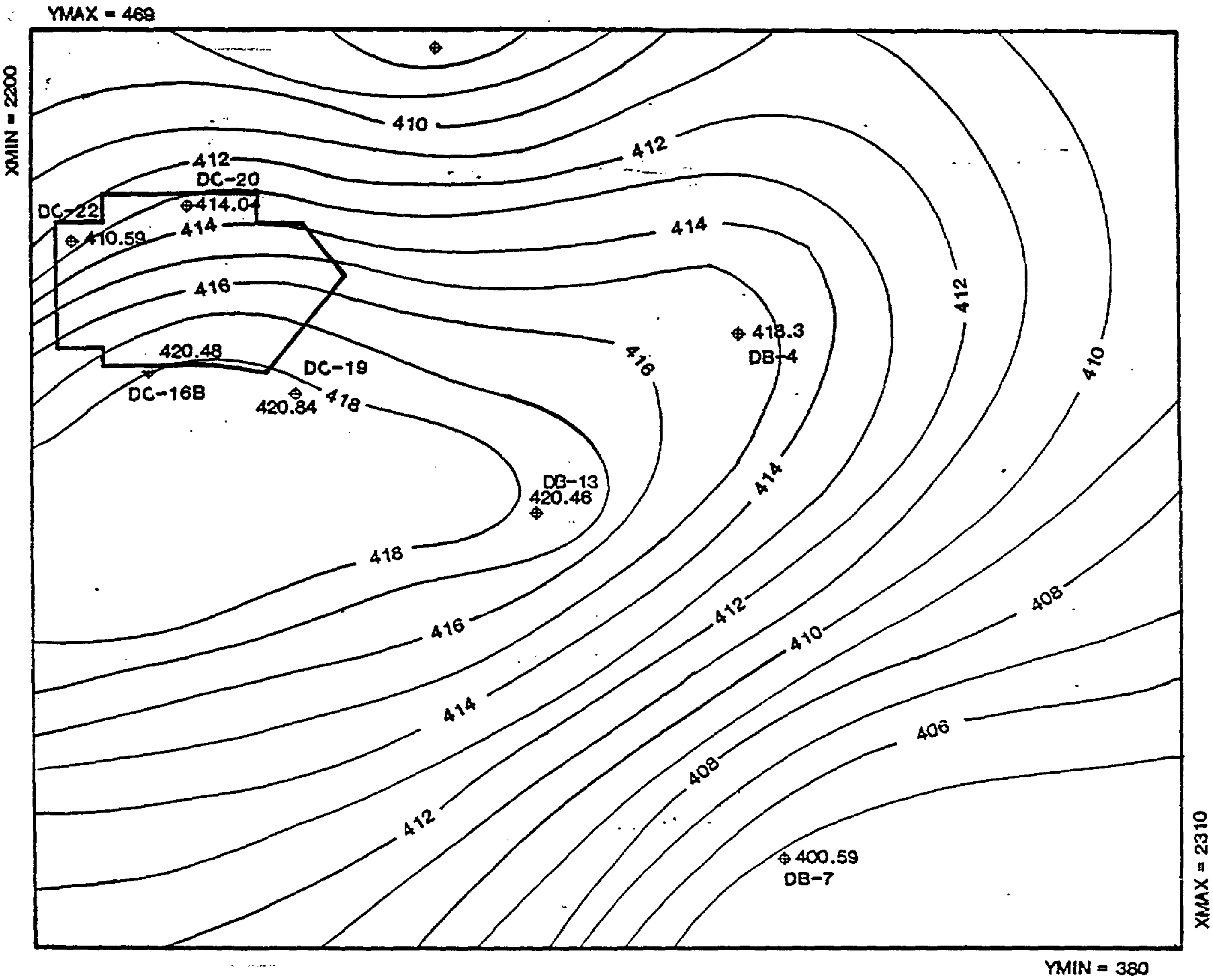

FIGURE 13: MABTON INTERBED
MAP OF HEAD ELEVATIONS

ENGINEERING FOR EARTH • WATER • AIR RESOURCES

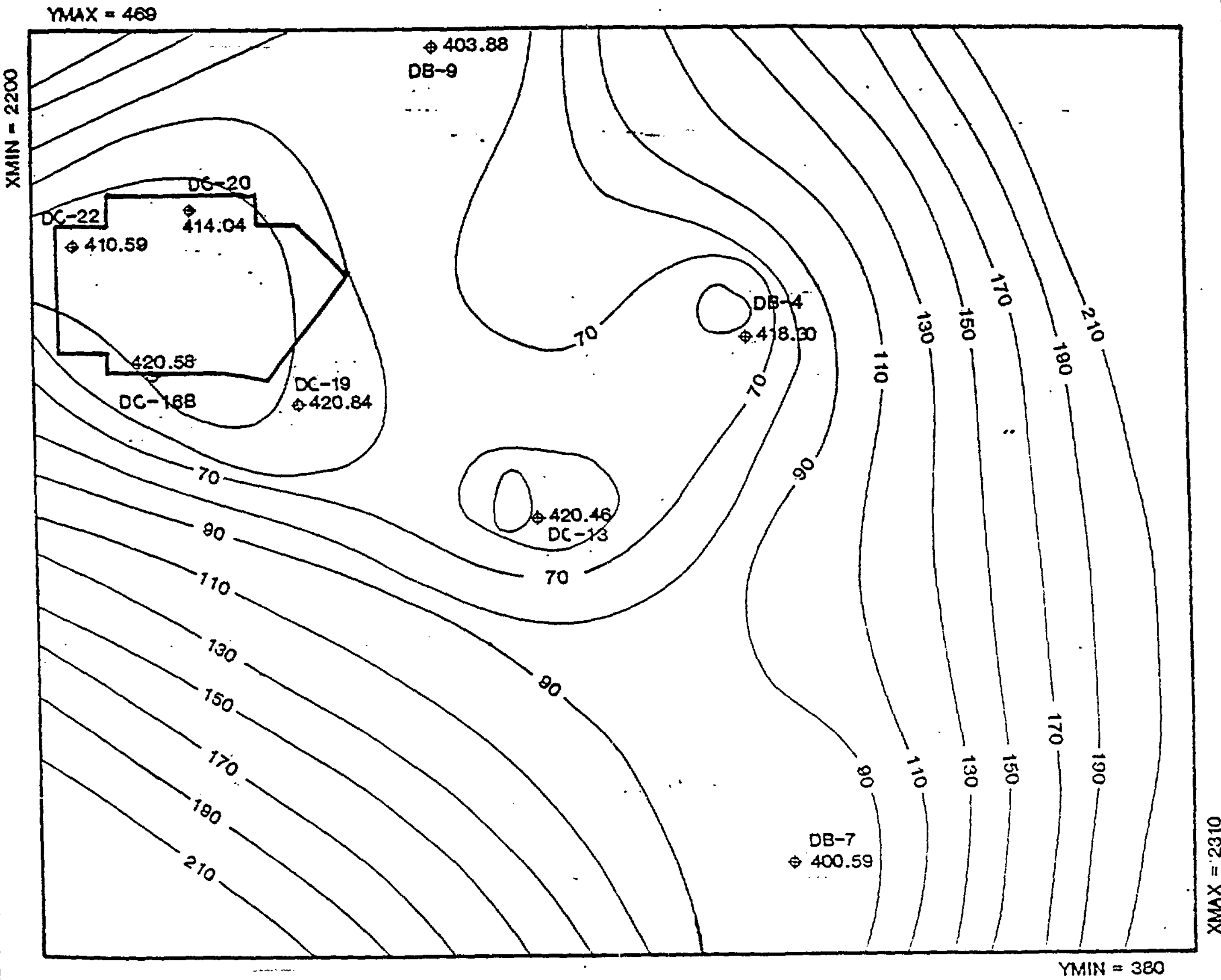

FIGURE 14: MABTON INTERBED
VARIANCE OF ESTIMATION ERROR

ENGINEERING FOR EARTH • WATER • AIR RESOURCES